Quantitative analysis of albumin uptake and transport in the rat microvessel endothelial monolayer

THERESA A. JOHN,[1] STEPHEN M. VOGEL,[1] CHINNASWAMY TIRUPPATHI,[1]
ASRAR B. MALIK,[1] AND RICHARD D. MINSHALL[1,2]
*Departments of [1]Pharmacology and [2]Anesthesiology, College of Medicine,
University of Illinois, Chicago, Illinois 60612*

John, Theresa A., Stephen M. Vogel, Chinnaswamy
Tiruppathi, Asrar B. Malik, and Richard D. Minshall.
Quantitative analysis of albumin uptake and transport in the
rat microvessel endothelial monolayer. *Am J Physiol Lung
Cell Mol Physiol* 284: L187–L196, 2003; 10.1152/ajplung.
00152.2002.—We determined the concentration depen-
dence of albumin binding, uptake, and transport in conflu-
ent monolayers of cultured rat lung microvascular
endothelial cells (RLMVEC). Transport of ^{125}I-albumin in
RLMVEC monolayers occurred at a rate of 7.2 fmol $\cdot$min^{-1} $\cdot$
10^6 cells^{-1}. Albumin transport was inhibited by cell surface
depletion of the 60-kDa albumin-binding glycoprotein gp60
and by disruption of caveolae using methyl-β-cyclodextrin.
By contrast, gp60 activation (by means of gp60 cross-linking
using primary and secondary antibodies) increased ^{125}I-al-
bumin uptake 2.3-fold. At 37°C, ^{125}I-albumin uptake had a
half time of 10 min and was competitively inhibited by
unlabeled albumin (IC$_{50}$ $\approx$ 1 M). Using a two-site model, we
estimated by Scatchard analysis the affinity (K_D) and maxi-
mal capacity (B$_{max}$) of albumin uptake to be 0.87 M (K_{D1})
and 0.47 pmol/10^6 cells (B$_{max1}$) and 93.3 M (K_{D2}) and 20.2
pmol/10^6 cells (B$_{max2}$). At 4°C, we also observed two popula-
tions of specific binding sites, with high (K_{D1} $\approx$ 13.5 nM, 1%
of the total) and low (K_{D2} $\approx$ 1.6 M) affinity. On the basis of
these data, we propose a model in which the two binding
affinities represent the clustered and unclustered gp60
forms. The model predicts that fluid phase albumin in caveo-
lae accounts for the bulk of albumin internalized and trans-
ported in the endothelial monolayer.

capillary permeability; vesicular transport; caveolae; albu-
min-binding glycoprotein gp60

THERE IS ACCUMULATING EVIDENCE from morphological
and functional studies that albumin is continuously
exchanged between the microvascular and intersti-
tial compartments by receptor-mediated albumin
transcytosis (8, 11, 13, 16–19, 23, 27–29). Recent
studies show that albumin molecules can associate
with surface glycoproteins such as gp60 (albondin) in
endothelial cells, which can activate the transport of
albumin (2, 6–8, 13, 19, 20, 23, 25, 28, 29). The
signaling pathways mediating transcytosis are not
well understood. The pathway involving the hetero-
trimeric G protein G_i and the activation of *Src* kinase
signaling may activate albumin endocytosis and its
transport from the luminal to the abluminal cell
surface (12–14, 27). Interestingly, albumin transcy-
tosis was augmented by antibody-induced cross-link-
ing of gp60 (13, 27–29). These studies suggest that,
under physiological conditions, albumin can bind to
its cell surface receptors [the albumin-binding pro-
teins (ABPs)] and initiate transcytosis.

However, important issues concerning the mode of
albumin uptake and transport by a transcellular
route remain unresolved. Fluid phase transport of
albumin in vesicles or via the paracellular pathway
would not be expected to be a saturable process,
whereas transport of albumin, either bound to recep-
tors or regulated by receptors, should be saturable.
In addition, the high-affinity nature of ABPs such as
gp60 (in the nanomolar range) (19, 25) relative to
plasma and interstitial concentrations of albumin
($\approx$1 mM) implies that *1*) albumin uptake and trans-
cytosis should be constitutive processes and *2*) bound
albumin may not dissociate from its vesicular carri-
ers upon exocytosis. These questions could not be
previously addressed with any rigor, because deter-
minations of affinity of albumin to the endothelial
plasmalemma were hampered by high nonspecific
binding (2, 6, 7, 19). This masked any saturable and
specific albumin binding. In the present study, we
determined the concentration dependency of albu-
min binding on the surface of confluent endothelial
monolayers and transport of albumin. We specifi-
cally used cultured rat lung microvascular endothe-
lial cells (RLMVEC), because they were shown by us
to have low nonspecific cell surface adsorption of
albumin. We show that *1*) binding and uptake of
albumin have saturable and fluid phase components,
2) cellular uptake of albumin is submaximal at phys-
iological serum albumin concentration, implying
that it can be further increased in response to appro-
priate signals, and *3*) gp60, an ABP, can activate
albumin transport.

Address for reprint requests and other correspondence: R. D.
Minshall, University of Illinois at Chicago, Dept. of Pharmacology
(m/c 868), 835 S. Wolcott Ave., Chicago, IL 60612 (E-mail:
rminsh@uic.edu).

METHODS

Endothelial Cell Cultures

RLMVEC (VEC Technologies, Rensselaer, NY) were cultured in high-glucose DMEM (GIBCO BRL, Grand Island, NY) supplemented with 5% fetal bovine serum (Hyclone, Logan, UT) plus 50 U/ml penicillin and 50 g/ml streptomycin, as described previously (4). The cultures were maintained in 5% CO_2-95% room air at 37°C.

Drugs and Reagents

All drugs and reagents were obtained from Sigma Chemical (St. Louis, MO) unless stated otherwise. Hanks' balanced salt solution (HBSS) containing $NaHCO_3$ (4.2 mM) and HEPES (10 mM) was adjusted to pH 7.4. Bovine serum albumin (fraction V, 99% pure, endotoxin free, cold alcohol precipitated) was freshly dissolved in HBSS in concentrations of 0.01–100 mg/ml. Methyl-ffi-cyclodextrin was dissolved in HBSS. Rabbit antibody against bovine endothelial gp60 (anti-gp60 antibody) was prepared and labeled with Cy3, as described elsewhere (25, 27). Control isotype-matched antibody was isolated from rabbit preimmune serum. Monoclonal anti-caveolin-1 antibody was obtained from Transduction Laboratories (Lexington, KY). Goat anti-mouse IgG labeled with Alexa 568 or 350, bovine serum albumin-Alexa 488 conjugate, and cholera toxin subunit B-Alexa 594 conjugate were purchased from Molecular Probes (Eugene, OR).

Albumin Iodination

Labeling of albumin with Na-[125]I (ICN Pharmaceuticals) was performed using chloramine T (3). The tracer albumin formed was purified to 0.4% free ^{125}I using Sephadex G-25 columns (Sigma Chemical). Specific radioactivity was 0.3 −1.0 Ci/ g albumin determined by 10% trichloroacetic acid precipitation.

Methyl-ff-Cyclodextrin Treatment

Confluent RLMVEC monolayers were incubated with methyl-ffi-cyclodextrin (0.2 nM–10 mM) in HBSS for 15 min, washed twice with HBSS, and incubated with fresh medium containing tracer albumin for the desired periods.

Immunostaining

Cellular localization of albumin, gp60, and caveolin-1 in the plasma membrane and plasmalemmal vesicles exposed to albumin was determined by immunocytochemical labeling and laser scanning confocal microscopy (LSM 510, Zeiss). RLMVEC were serum deprived for 2 h, washed three times with HEPES-buffered HBSS or phenol red-free DMEM, and exposed to 0.1 mg/ml albumin in the presence of 50 g/ml Alexa 488-conjugated albumin, 20 g/ml cholera toxin subunit B-Alexa 594 conjugate, and/or 3.5 g/ml Cy3-anti-gp60 antibody for up to 30 min (13). Cells were then washed three times with HBSS, fixed with 4% paraformaldehyde in HBSS, and blocked for 30 min in HBSS containing 5% goat serum, 0.1% Triton X-100, and 0.01% NaN_3. Primary antibody labeling was performed overnight at 4°C with anti-caveolin-1 antibody (1 g/ml). Coverslips were then washed three times for 10 min in HBSS, blocked for 30 min with 5% goat serum, and incubated for 2 h at room temperature with fluorescent-labeled goat anti-rabbit and goat anti-mouse secondary antibody. In some cases, 4,6-diamidino-2-phenylindole dihydrochloride (DAPI, 1 g/ml) was added to visualize the nucleus. Confocal microscopy was performed using 364-, 488-, and 568-nm excitation laser lines to detect DAPI/Alexa 350 (band pass 385−470 nm emission), FITC/Alexa 488 (band pass 505–550 nm emission), and rhodamine/Alexa 568 fluorescence (long pass 585 nm emission) in optical sections 1 m thick (pinhole set to achieve 1 Airy unit).

Cell Surface gp60 Cross-Linking

RLMVEC monolayers were washed twice with HEPES-buffered DMEM at 4°C and incubated for 30 min at 4°C with anti-gp60 antibody (20 g/ml) and then with secondary antibody (goat anti-rabbit, 20 g/ml) for 30 min to cross-link gp60. Controls were treated with the preimmune antibody (20 g/ml) at 4°C for 30 min. Cells were rewarmed to 37°C to activate endocytosis (27). To deplete ABP gp60 (27), anti-gp60 antibody was preincubated with cells for 2 h at 37°C.

Binding of ^{125}I-Albumin

Confluent cell cultures in six-well plates (1.0–1.2 10^6 cells/35 mm) were washed twice in 10 mM HEPES-buffered DMEM, pH 7.4, and then serum deprived for 2 h by incubation in DMEM. Cells were precooled to 4°C for 30 min, and ^{125}I-albumin in the presence or absence of unlabeled albumin in HBSS was added for 30 min at 4°C. Unbound ligand was removed by three washes with ice-cold HBSS, and cells were lysed with 1 ml of 50 mM Tris fHCl buffer, pH 7.4, containing 1% Triton X-100 and 0.5% SDS (13). Cell-associated ^{125}I-albumin counts were measured in a gamma counter (Packard Instruments, Downers Grove, IL).

Uptake of ^{125}I-Albumin

Serum-deprived confluent RLMVEC monolayers (see above) were pretreated with indicated reagents at 37°C for required periods before addition of ^{125}I-albumin in the presence or absence of unlabeled albumin in HBSS. Uptake at 37°C was allowed to proceed for times indicated and then terminated by chilling on ice and washing three times with ice-cold HBSS. To remove cell surface-bound ^{125}I-albumin, cells were washed three times with 1 ml of acid wash buffer (0.5 M NaCl and 0.2 M acetic acid, pH 2.5) (26). Cells were then lysed and counted as described above.

Transendothelial ^{125}I-Albumin Transport

RLMVECs were grown on clear microporous polyester Transwell membranes (12 mm diameter, 1 cm^2 growth area, 0.4 m pore size; Corning Costar, Cambridge, MA). The membrane inserts were filled with a total of 0.5 ml of incubate containing ^{125}I-albumin in the presence or absence of unlabeled albumin. The lower well was filled with 1.5 ml of incubate of the same osmolarity as the inner well. Thus fluid levels and osmotic pressure in the "upper" and "lower" wells were equalized to minimize hydrostatic and osmotic effects. Labeled albumin and test agents were added to the upper well in equimolar solution, and transendothelial ^{125}I-albumin permeability was measured at 37°C. Aliquots of 50 l were sampled from the lower chamber every 10–15 min, and gamma radioactivity was measured. Albumin permeability was calculated for radiolabeled albumin flux across the cell monolayer, as described elsewhere (5, 22). Trichloroacetic acid precipitation analysis and SDS-PAGE of the tracer albumin (27) in the abluminal chamber showed that the radioactivity measured on the abluminal side of the cell monolayer remained attached to albumin and that albumin was not hydrolyzed in the uptake or transport process.
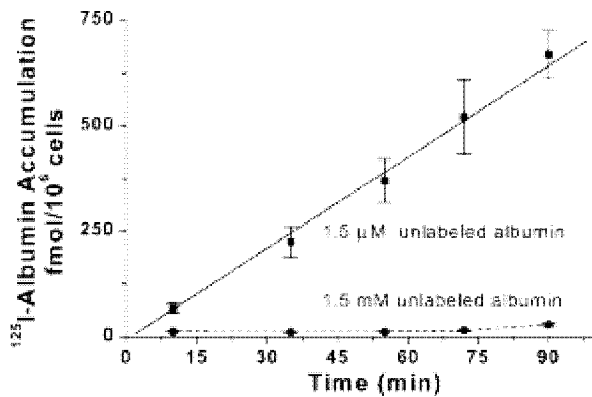
Fig. 1. Time course of transendothelial ^{125}I-albumin permeability. ^{125}I-Albumin transport was determined in rat lung microvascular endothelial cells (RLMVEC) grown to confluence in Transwell inserts. Tracer albumin (68 nM ^{125}I-albumin) was applied to the apical chamber together with 1.5 M or 1.5 mM free albumin, which was also present in the basal chamber to equalize osmotic pressure, and samples from the basal chamber were taken every 10–15 min for 90 min (4 wells per incubation time). Specific transport of ^{125}I-albumin (amount inhibited by 1.5 mM albumin) was 80% of total ^{125}I-albumin clearance. ^{125}I-Albumin transport was cumulative, increasing linearly for up to 90 min. Data are from 1 experiment, which is representative of 3 experiments performed.

Statistical Analysis

Data were analyzed by the nonlinear least-squares curve-fitting programs LIGAND (Elsevier Biosoft) and Microcal Origin (Microcal Software, Northhampton, MA). Student's *t*-test was used to compare results at significance level of P 0.05. Multiple comparisons were made by ANOVA. All statistical tests were made using GraphPad Prism Instat software (San Diego, CA).

RESULTS

Albumin Transport in Endothelial Monolayers

Time course of transendothelial ^{125}I-albumin transport. For studies of transendothelial ^{125}I-albumin transport in the apical-to-basolateral direction, RLMVEC were grown to confluence on Transwell filter inserts (1-cm^2 surface area). Experiments began when the liquid in the upper well was replaced by a warm (37°C) solution containing ^{125}I-albumin plus unlabeled albumin (1.5 M or 0.1 mg/ml). During the 90-min period, aliquots of media (0.05 ml) in the lower well were sampled and analyzed for gamma radioactivity (see METHODS). Appearance of tracer albumin in the basal chamber vs. time described a straight line (Fig. 1), as predicted if the backflux of tracer (into upper chamber) was negligible. From the slope of the fitted line in Fig. 1, we calculated the ^{125}I-albumin flux of 7.2 fmol·min[ff1]·10^6 cells[ff1]. Excess unlabeled albumin (1.5 mM or 100 mg/ml) blocked ^{125}I-albumin flux (Fig. 1), implying competition between labeled and unlabeled albumin at the apical endothelial plasmalemmal surface.

Cell pathway regulates albumin transport. The effect of methyl-ffi-cyclodextrin, the cholesterol-binding agent that disrupts caveolae (10), on transendothelial ^{125}I-albumin permeability was assessed. RLMVEC mono-

layers grown on Transwell filter inserts received vehicle (without drug) or methyl-ffi-cyclodextrin (0.2 nM –10 mM) for 15 min in the upper chamber, and tracer albumin was added immediately thereafter. Methyl-ffi-cyclodextrin blocked transendothelial ^{125}I-albumin permeability with an IC$_{50}$ of 1.0 M (Fig. 2). The highest concentration of the inhibitor (10 mM) reduced permeability of the albumin tracer by 80% (from 7.7 to 1.5 fmol·min[ff1]·ff10^6 cells[ff1]), indicating the importance of the cellular pathway in albumin transport in RLMVEC.

Regulation of transendothelial albumin transport by gp60. Inasmuch as activation of gp60 can stimulate albumin endocytosis in endothelial cells via caveolae (13, 21, 27), we determined whether gp60 activation also increased the transport of tracer albumin. To prevent internalization of the antigen-antibody complex, gp60 on the apical cell surface was cross-linked, as described elsewhere (27), using an anti-gp60 antibody for 30 min in cold conditions (4°C). Cells were rapidly rewarmed to 37°C with a solution containing ^{125}I-albumin (2.5 nM) plus unlabeled albumin (1.5 M) to activate uptake of the tracer. Control cultures received isotype-matched antibody in lieu of anti-gp60 antibody. Cross-linking of gp60 significantly increased ^{125}I-albumin permeability 2.3-fold above the control value of 38 1.5 nl·min[ff1]·ffcm[ff2]. Excess unlabeled albumin (1 mM) reduced ^{125}I-albumin permeability to 1.2 0.6 nl·min[ff1]·ffcm[ff2] (Fig. 3) in the cells subjected to gp60 cross-linking. To address the dependence of basal transport of tracer albumin on the cell surface gp60, RLMVEC monolayers were incubated with anti-gp60 antibody for 2 h at 37°C to deplete cell surface gp60 (9, 27). This procedure reduced basal transendothelial ^{125}I-albumin permeability to 7.3 0.6 nl·min[ff1]·ffcm[ff2] (80% inhibition; Fig. 3).
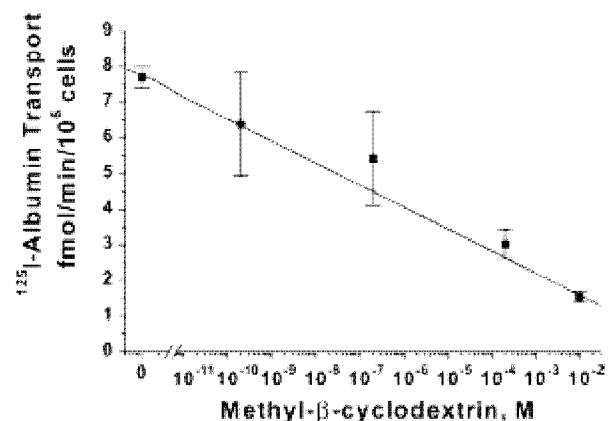

Fig. 2. Inhibitory effect of methyl-ffi-cyclodextrin on flux of ^{125}I-albumin. RLMVEC on Transwell inserts were preincubated for 15 min with 0.2 nM –10 mM methyl-ffi-cyclodextrin or vehicle and then with ^{125}I-albumin in Hanks' balanced salt solution (HBSS) containing 1.5 M free albumin for 15 min. A dose-dependent inhibition of ^{125}I-albumin flux from a control value of 7.7 0.3 fmol·min[ff1]·ff10^6 cells[ff1] was observed. Values are means SE from 4 replicates for each point in 1 experiment, which is representative of 4 experiments performed.
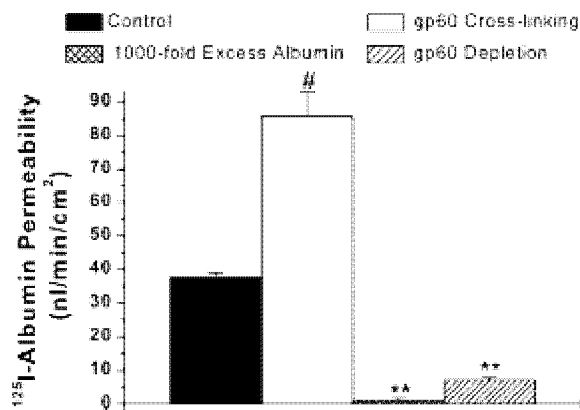
Fig. 3. 60-kDa albumin-binding protein (gp60)-dependent ^{125}I-albu -
min transport in RLMVEC. RLMVEC monolayers were washed
twice with HEPES-buffered DMEM at 4°C and incubated for 30 min
with anti-gp60 antibody (10 g/ml) at 4°C and with secondary anti-
body (goat anti-rabbit, 10 g/ml) for 30 min to induce cross-linking.
Controls were treated with preimmune antibody (10 g/ml) and
secondary antibody. Cells were rewarmed to 37°C to activate uptake
of ^{125}I-a bumin and 1.5   M unlabeled albumin. Cross-linking of gp60
increased ^{125}I-albumin permeability 2.3-fold from a control value of
38   15 nl ffmin^{ff1} fbm^{ff2} . To deplete cell surface gp60, RLMVEC
monolayers were washed twice with HEPES-buffered DMEM and
incubated with anti-gp60 antibody (10 g/ml) for 2 h at 37 °C. Deple-
tion of gp60 reduced ^{125}I-albumin transport by 85%. ^{125}I-Albumin
flux was also blocked by 95% when cells were coincubated with 1.5
mM unlabeled albumin (100 mg/ml). Values are means   SE (n ffl 4).
$^{#,**}P$ 0.01 vs. control by ANOVA.

Albumin Uptake in Endothelial Cell Monolayers

Time course of tracer albumin uptake. RLMVEC
monolayers were incubated for various periods with
^{125}I-albumin in the presence of 1.5   M unlabeled albu -
min. ^{125}I-albumin accumulation within the cells was
determined by counting gamma radioactivity in cell
lysates. Lysates were prepared from acid-washed cells
to avoid contamination by tracer albumin associated
with the cell exterior. The time course of cellular ^{125}I-
albumin uptake was biphasic (Fig. 4). Specific tracer
uptake (^{125}I-albumin uptake in the presence of 1.5   M
albumin minus that in 1.5 mM albumin) reached an
initial peak (60 fmol/10^6 cells) within   15 min, ap-
proached a minimum (50 fmol/10^6 cells) at 30–45 min,
and finally rose to a second peak (75 fmol/10^6 cells) at
75 min. The initial slope of the uptake curve was used
to estimate the rate of tracer albumin uptake, which
was 6 fmol ffmin^{ff1} ffl0^6 cells^{ff1} ; this value was within
the same range as ^{125}I-albumin transendothelial trans   -
port of 7.2 fmol ffmin^{ff1} ffl0^6 cells^{ff1} (see above). Endo-
thelial ^{125}I-albumin uptake was markedly inhibited at
each time point by excess (1.5 mM) unlabeled albumin
(Fig. 4).

Concentration dependence of albumin uptake. Sub-
maximal concentrations of unlabeled albumin pro-
duced biphasic inhibition of tracer albumin uptake
(Fig. 5A; I C$_{50}$ ffl 1.15   M). Scatchard analysis (Fig. 5B)
used to parse the sigmoidal function into its two com-
ponents showed a 0.87   M high-affinity component,
with maximal binding capacity (B$_{max}$) ffl 0.47 pmol/10^6
cells, and a 93.3   M low-affinity component, with

B$_{max}$ ffl 20.2 pmol/10^6 cells. From these data, we deter-
mined the total albumin uptake (labeled   unlabeled
forms) as a function of albumin concentration (Fig. 5   C).
The cellular uptake of albumin was dependent on al-
bumin concentration; the steepest region of concentra-
tion dependency was between 10^{ff5} and 10^{ff3} M albu-
min. The smooth curve in Fig. 5C predicts an EC$_{50}$ of
  100   M and saturation of transport at   3 mM albu-
min.

Confocal fluorescence imaging of albumin uptake. We
visualized the uptake of albumin in caveolae by colo-
calization of fluorescent forms of albumin, cholera
toxin subunit B, and anti-gp60 antibody. Cholera toxin
subunit B was used as a specific marker for caveolae,
because it labels the caveolae-specific ganglioside GM1
(14); gp60 was previously shown to be associated with
endothelial caveolae (13). After 30 min of incubation
with these fluorescent probes at 37°C, cells were acid
washed to remove residual cell surface probe, fixed,
and stained with the nuclear marker DAPI (1 g/ml) or
anti-caveolin-1 antibody plus Alexa 350-labeled sec-
ondary antibody. High-resolution confocal images
(1.0   m optical thickness) in Fig. 6A show internal-
ized Alexa 488-albumin and Cy3-gp60 antibody, to-
gether with caveolin-1 immunostaining near the apical
cell surface. Coincident staining of gp60 and albumin
and colocalization of all three probes were apparent in
the overlay. In other experiments, fluorescent albumin
was coincubated with fluorescent cholera toxin subunit
B. Figure 6B shows the confocal images of internalized
Alexa 594-cholera toxin subunit B and Alexa 488-albu-
min, together with DAPI. The fluorescence of albumin
and cholera toxin was coincident in the merged image,
indicating albumin 's association with caveolae.

To address the effects of methyl- ffi-cyclodextrin on
albumin uptake and caveolin-1 distribution, endothe-
lial cells were pretreated with 10 mM methyl- ffi-cyclo-
dextrin and incubated with HBSS containing Alexa
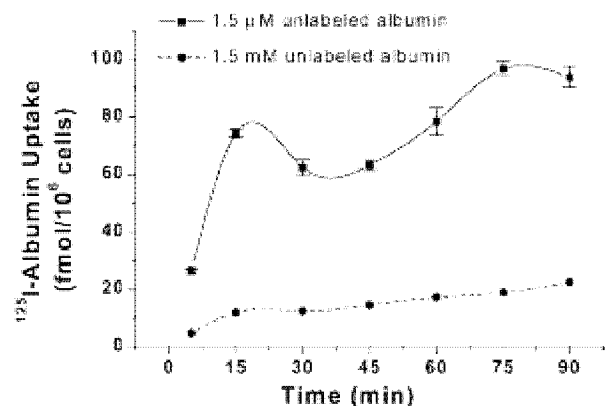

Fig. 4. Time course of endothelial ^{125}I-albumin uptake. Confluent
RLMVEC were incubated for 5–90 min (6 wells per incubation time)
with 22.8 nM ^{125}I-a bumin and 1.5   M albumin to quantify total
uptake (*) or with 1.5 mM unlabeled a bumin to quantify nondis-
placeable ^{125}I-a bumin uptake (F). Total uptake of ^{125}I-albumin in -
creased with time, peaking initially   at 15 min and again at 75 min
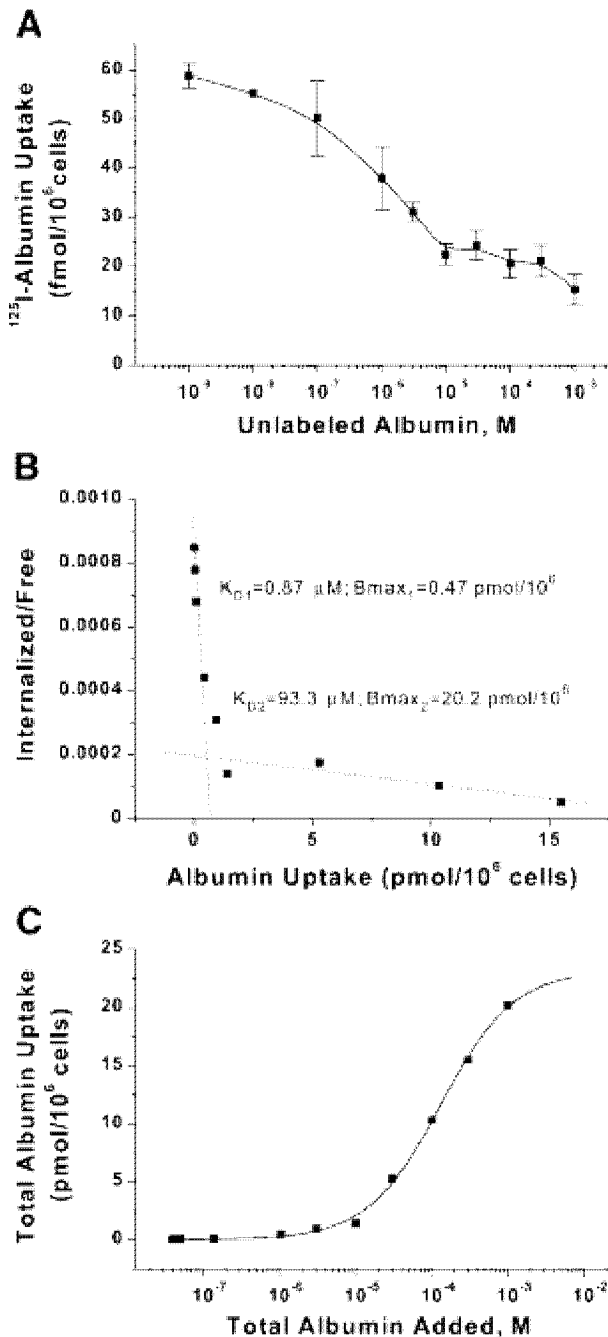(half time ffl 10 min). Data are representative of 4 separate experi-
ments.

Fig. 5. Competition kinetics of ^{125}I-albumin uptake by unlabeled albumin. Increasing concentrations of unlabeled albumin (10^{ff9} – 10^{ff3} M) were added to RLMVEC monolayers followed by 34 nM ^{125}I-albumin, and monolayers were incubated at 37°C for 1 h. *A*: uptake of ^{125}I-albumin was inhibited in the presence of increasing concentrations of free albumin. IC_{50} was calculated to be 1.15 M; near-maximal displacement was achieved with 1 mM a bumin. *B*: Scatchard analysis of ^{125}I-albumin displacement was best fit b y a 2-site model, represented by K_{D1} and B_{max1} (*site 1*) and K_{D2} and B_{max2} (*site 2*), where K_D is affinity constant and B_{max} is maximal binding capacity. *C*: total a bumin uptake calculated from Scatchard analysis of combined tracer ^{125}I-a bumin plus unlabeled albumin uptake shows saturation of albumin uptake with   3 mM added albumin. Data are representative of 4 separate experiments.

488-tagged albumin (50   g/ml) plus unlabeled albumin (1.5   M) for 30 min. Cells were acid washed, fixed, and stained for nuclei (DAPI) and for caveolin-1 (i.e., anti-caveolin-1 monoclonal antibody at 1   g/ml followed by goat anti-mouse Alexa 568-labeled secondary anti-body). Methyl-ffi-cyclodextrin   abolished albumin inter-nalization by plasmalemmal vesicles (Fig. 7). In addi-tion, methyl-ffi-cyclodextrin   markedly reduced the cell surface-associated caveolin-1 immunostaining, consis-tent with its effect in disrupting cell surface caveolae.

Albumin Binding to Endothelial Cell Surface

Competition between endothelial cell surface labeled and unlabeled albumin. Agonist competition binding studies were made using RLMVEC in cold conditions (4°C) to abolish tracer endocytosis and internalization. Cells were incubated with ^{125}I-albumin in the presence or absence of unlabeled albumin (10^{ff12} –10^{ff3} M) for 30 min. Unlabeled albumin reduced the specific binding of ^{125}I-albumin from 17.5 to 2.7   0.4 fmol/10^6 cells. The IC_{50} and Hill coefficient fitted to the data were 4.5 nM and 0.28, respectively, suggesting the existence of more than one albumin binding site on the RLMVEC surface (Fig. 8*A*). Scatchard analysis of the binding data (Fig. 8*B*) demonstrated two albumin binding sites, with af-finity (K_D) values of 13.5 nM and 1.6   M, respectively, and corresponding B_{max} values of 24.2 fmol/10^6 cells and 2.4 pmol/10^6 cells. The lower-af finity site ac-counted for   98% of the binding.

Displacement of albumin from cell surface binding sites by anti-gp60 antibody. Pretreatment of RLMVEC monolayers for 1 h at 4°C with a 1:200 dilution of anti-gp60 antibody decreased ^{125}I-albumin binding by 47.8   5.1% (*n* ffl 3) relative to control antibody. The tracer albumin and the specific anti-gp60 antibody competed for the same membrane binding sites. Thus high- and low-affinity binding sites detected on RLM-VEC may represent different states of gp60.

DISCUSSION

RLMVEC monolayers exhibited a high degree of specific ^{125}I-albumin binding, because   80% of total binding was inhibited by excess unlabeled albumin. Although a saturable low-af finity binding site for albu-min has been described in bovine pulmonary artery endothelial cells (23) and rat fat tissue microvessel endothelial cells (20), the finding of a second site of much higher affinity is a novel observation. Competi-tion studies of ^{125}I-albumin binding under cold condi-tions (4°C) to prevent tracer internalization   showed that albumin bound to the endothelial cell surface with affinity constants of 13.5 nM (K_{D1}) and 1.6   M (K_{D2}). On the basis of the corresponding B_{max} values, the high-affinity site represented   1% of the specific albu-min binding and averaged 5 10^5 sites/cell. Schnitzer and Oh (21) and Tiruppathi et al. (25) demonstrated that an anti-gp60 antibody displaced the specific bind-ing of ^{125}I-albumin from rat and bovine pulmonary microvascular endothelial cells, consistent with our

DOCKET ALARM

Explore Litigation Insights

Docket Alarm provides insights to develop a more informed litigation strategy and the peace of mind of knowing you're on top of things.

Real-Time Litigation Alerts

Keep your litigation team up-to-date with **real-time alerts** and advanced team management tools built for the enterprise, all while greatly reducing PACER spend.

Our comprehensive service means we can handle Federal, State, and Administrative courts across the country.

Advanced Docket Research

With over 230 million records, Docket Alarm's cloud-native docket research platform finds what other services can't. Coverage includes Federal, State, plus PTAB, TTAB, ITC and NLRB decisions, all in one place.

Identify arguments that have been successful in the past with full text, pinpoint searching. Link to case law cited within any court document via Fastcase.

Analytics At Your Fingertips

Learn what happened the last time a particular judge, opposing counsel or company faced cases similar to yours.

Advanced out-of-the-box PTAB and TTAB analytics are always at your fingertips.

API

Docket Alarm offers a powerful API (application programming interface) to developers that want to integrate case filings into their apps.

LAW FIRMS
Build custom dashboards for your attorneys and clients with live data direct from the court.

Automate many repetitive legal tasks like conflict checks, document management, and marketing.

FINANCIAL INSTITUTIONS
Litigation and bankruptcy checks for companies and debtors.

E-DISCOVERY AND LEGAL VENDORS
Sync your system to PACER to automate legal marketing.

fastcase®
Smarter legal research.